Development, Growth & Differentiation
The Japanese Society of Developmental Biologists
Develop. Growth Differ. (2016) **58**, 600–608 doi: 10.1111/dgd.12301

Original Article

Abnormal spermatogenesis and male infertility in testicular zinc finger protein *Zfp318*-knockout mice

Masamichi Ishizuka,[1] Eri Ohtsuka,[1] Atsuto Inoue,[1] Mirei Odaka,[1] Hirotaka Ohshima,[1] Norihisa Tamura,[1] Kaoru Yoshida,[2] Norihisa Sako,[3] Tadashi Baba,[4] Shin-ichi Kashiwabara,[4] Masaru Okabe,[5] Junko Noguchi[6] and Hiromi Hagiwara[1,3]*

[1]*Department of Biological Sciences, Tokyo Institute of Technology, Yokohama 226-8501;* [2]*Biomedical Engineering Center, Toin University of Yokohama, Yokohama 225-8503;* [3]*Department of Biomedical Engineering, Toin University of Yokohama, Yokohama 225-8503;* [4]*Graduate School of Life and Environmental Sciences, University of Tsukuba, Ibaraki 305-8572;* [5]*Genome Information Research Center, Research Institute for Microbial Diseases, Osaka University, Osaka 565-0871; and* [6]*Germ Cell Conservation Laboratory, National Institute of Agrobiological Sciences, Ibaraki 305-8602, Japan*

Zfp318, a mouse gene with a Cys2/His2 zinc finger motif, is mainly expressed in germ cells in the testis. It encodes two alternative transcripts, which regulate androgen receptor-mediated transcriptional activation or repression by overexpression of them. However, the role of *Zfp318* is still obscure *in vivo*, especially in spermatogenesis. To elucidate the role of *Zfp318* during gamete production, we established a knockout mouse line. *Zfp318*-null male mice exhibited infertility, whereas *Zfp318*-null female mice displayed normal fertility. ZFP318 was expressed during multiple stages of spermatogenesis, from spermatocytes to round spermatids. The nuclei of secondary spermatocytes showed high levels of expression. Histological analysis and quantitative analysis of DNA content showed decreased numbers of both spermatids in the seminiferous tubules and mature spermatozoa in the epididymides of *Zfp318*-null mice. These results suggest that *Zfp318* is expressed as a functional protein in testicular germ cells and plays an important role in meiosis during spermatogenesis.

Key words: male infertility, sperm count, spermatogenesis, testis, zinc finger.

Introduction

Spermatogenesis is a complicated, well-coordinated process, with a gene expression program that uses both transcriptional and translational mechanisms (Sassone-Corsi 1997; Eddy 2002). Despite the expression of a large number of different transcription factors in male germ cells, few have been reported to have functional significance in spermatogenesis (Eddy 2002). According to more recent reports with gene knockout technology, *Zbtb16*/PLZF (Buaas *et al.* 2004; Costoya *et al.* 2004), *Sox3* (Weiss *et al.* 2003; Raverot *et al.* 2005), and *Sohlh1* (Ballow *et al.* 2006) are essential for spermatogonial stem cell self-renewal and mitosis during spermatogenesis. In post-meiotic germ cell development, CREM-τ acts as a switch that regulates the expression of genes required for haploid germ cell development (Blendy *et al.* 1996; Nantel *et al.* 1996). TATA box-binding protein-like 1 (TBPL1) is also required for spermiogenesis, and inactivation of TBPL1 results in complete arrest of spermiogenesis at step 7 in stage VII seminiferous tubules (Martianov *et al.* 2001).

Testicular zinc finger protein, TZF, is a polypeptide comprising 924 amino acid residues. It contains a Cys2/His2 zinc finger motif at the C-terminal end (Inoue *et al.* 2000), and its transcript is expressed during spermatogenesis (Ishizuka *et al.* 2003). We designated the gene as TZF, which is herein referred to as

*Author to whom all correspondence should be addressed.
Email: hagiwara@toin.ac.jp
Received 7 November 2015; revised 7 May 2016; accepted 23 May 2016.

Zfp318 according to the Mouse Genome Informatics nomenclature. Several Cys2/His2 zinc finger proteins are also expressed at specific stages during mouse spermatogenesis. For example, deficiency of ZFP105 in pachytene spermatocytes resulted in undifferentiated spermatogenic cells and decreased male fertility (Zhou *et al.* 2010). Ovol2/MOVO may play an important role in the XY body during spermatogenesis, possibly in XY body formation and meiotic sex chromosome inactivation (Chizaki *et al.* 2012). *Gtsf1/Cue110* is required for spermatogenesis and is involved in retrotransposon suppression in male germ cells (Yoshimura *et al.* 2009). *Zmynd15* was recently identified as a transcriptional repressor that was essential for spermiogenesis (Yan *et al.* 2010). We previously showed that short-form ZFP318 homodimers act as transcriptional repressors in the regulation of androgen receptor (AR)-mediated gene transcriptional activation (Ishizuka *et al.* 2005; Tao *et al.* 2006a,b). Interestingly, long-form ZFP318, an alternative splice variant of *Zfp318*, can form both homodimers and heterodimers with short-form ZFP318 and acts as a transcriptional activator of AR-mediated gene transcription. It contains 2025 amino acid residues, and its 902°N-terminal amino acids are identical to those of short-form ZFP318. The mRNAs of both splice variants of *Zfp318* are highly expressed in mouse testes, especially in germ cells (Ishizuka *et al.* 2003). If both proteins colocalize in spermatocytes, transcriptional activation and repression may occur depending on the expression of other proteins. Our previous study showed that short-form ZFP318 recruits endogenous histone deacetylase 2 (HDAC2) to suppress AR transcriptional activation, while the long-form ZFP318 homodimer or heterodimer recruits a coactivator complex to activate AR-mediated transcription (Tao *et al.* 2006b). These results suggest that *Zfp318* might function in mouse spermatogenesis via AR-mediated gene transcriptional activation. However, the study of cell-specific AR knockout showed that deletion of the AR gene in mouse germ cells does not affect spermatogenesis and male fertility (Wang *et al.* 2009). Therefore, there is no direct evidence that *Zfp318* has any crucial role in germ cells in spermatogenesis.

To elucidate the function of *Zfp318* in spermatogenesis, we here first described the detailed expression pattern of *Zfp318* in mouse testes and established a *Zfp318* knockout mouse line. *Zfp318*-null mice exhibited male-specific sterility because of a defect in spermatogenesis. The loss of *Zfp318* appeared to affect meiosis specifically, resulting in a reduced number of haploid sperm cells. Our current findings support that *Zfp318* is important for mouse spermatogenesis.

Material and methods

Generation of mutant mice lacking Zfp318

The targeting strategy is shown in supplementary data (Fig. S1A). 129SvJ ES cell clones carrying the targeted mutation were injected into C57BL/6 blastocysts, and chimeric male mice were crossed with C57BL/6 females to establish heterozygous (*Zfp318*$^{+/-}$) mutant lines. We established the congenic strains of 129SvJ and C57BL/6, which lacked *Zfp318*, by backcrossing at least seven generations. Northern and Southern blot analyses confirmed *Zfp318* deletion (Fig. S1B,C). For breeding studies, wild-type (+/+), heterozygous (+/−), and homozygous (−/−) male mice (8–10 weeks old each; $n = 10$) were caged for 2 weeks with four females (8 weeks old, ddY mice) each, and pregnancies/deliveries were recorded. All animal experiments were performed according to the protocols approved by the Institutional Animal Care and Use Committee of Toin University of Yokohama.

Western blot analyses

Mouse testes from the congenic strain 129SvJ were homogenized by a POLYTRON Homogenizer (KINEMATICA AG, Lucerne, Switzerland) in TBS supplemented with cOmplete Protease Inhibitor Cocktail (EDTA-free) (Roche, Mannheim, Germany) and treated with Benzonase Nuclease (Novagen, Billerica, MA, USA). Proteins were separated by a NuPAGE SDS–PAGE Gel System using 3–8% Tris-Acetate Gels (Novex, Carlsbad, CA, USA) and transferred to PVDF membranes. The anti-ZFP318 antibody (human ZNF318 antibody; HPA027031, Sigma-Aldrich, Saint Louis, MO, USA), horse radish peroxidase (HRP)-conjugated anti-rabbit IgG (GE, Fairfield, CT, USA), and ECL Prime (GE) were used for the detection of ZFP318.

In situ *hybridization*

The digoxigenin (DIG) antisense and sense *Zfp318* riboprobes for *in situ* hybridization were synthesized using a DIG RNA Labeling Kit (Roche). The sequence positions which are specific to short and long transcripts of *Zfp318* were 2825–3122 and 5665–6157, respectively. After being perfused, congenic 129SvJ wild-type mouse testes were dissected, fixed with Tissue Fixative (Genostaff, Tokyo, Japan), and embedded in paraffin according to standard procedures. Paraffin blocks were sectioned

at 8-μm thickness. After being treated with proteinase K (10 μg/mL) for 30 min at 37°C, the sections were post-fixed in 4% paraformaldehyde for 10 min, washed with phosphate-buffered saline (PBS), and placed in 0.2 mol/L HCl for 10 min. Then, they were washed with PBS and acetylated by incubation in 0.1 mol/L triethanolamine and 0.25% acetic anhydride for 10 min. Hybridization was performed with probes at concentrations of 100 ng/mL in Probe Diluent (Genostaff) at 60°C for 16 h. After treatment with blocking reagent, the sections were incubated with alkaline phosphatase (AP)-conjugated anti-DIG antibodies (Roche) diluted 1:1000 with TBST for 2 h. The sections were visualized with BM Purple AP Substrate (Roche) overnight, and counterstained with Kernechtrot stain solution (Mutoh, Tokyo, Japan).

Immunohistochemical and histological analysis

The testes from congenic 129SvJ mice were dissected and fixed in Bouin's fixative for 2 h at room temperature (RT). The tissues were embedded in paraffin and then cut into 4-μm-thick sections. For immunohistochemical analysis, antigens were retrieved by heating in citrate buffer (pH 6.0), and sections were incubated with 10% goat serum (Nichirei, Tokyo, Japan) as blocking solution. The anti-ZFP318 antibody was diluted to 6 μg/mL in 10% goat serum. The sections were incubated with the antibody, washed, and incubated with secondary antibody (Simple Stain Mouse MAX PO, Nichirei). The AEC (3-amino- 9-ethylcarbazole) Substrate Kit (Nichirei) was applied until a red color developed. For histological analysis, spermatogenesis was examined in sections stained with hematoxylin and eosin (H&E) or PAS and hematoxylin. Photomicrographs were taken with the All-in-One Fluorescence Microscope system (BZ-8100 and BZ-Analyzer, Keyence). The seminiferous tubules were staged according to a reference (Russell *et al.* 1990).

Preparation of testicular and epididymal cells

Testicular and epididymal cells were prepared as previously described (Krishnamurthy *et al.* 2000). Briefly, the tissues were minced in PBS and gently aspirated to disperse the cells. The cell suspension was filtered through a 35-μm nylon mesh, and cells were washed in PBS. After centrifugation and aspiration, the cells were resuspended in PBS, fixed in 70% chilled ethanol, and stored at 4°C until further analysis. Cells from the cauda epididymis were prepared and stored in the same manner.

Quantification of testicular and epididymal cells by DNA flow cytometry

Mouse testicular and epididymal cells were stained essentially as described previously (Krishnamurthy *et al.* 1998). Briefly, an aliquot of 1×10^6 to 2×10^6 ethanol-fixed testicular and epididymal cells were washed with PBS and treated with 0.25% pepsin solution for 10 min at 37°C. After centrifugation, cells were stained with propidium iodide (PI) staining solution (25 μg/mL PI, 40 μg/mL RNase, and 0.3% Tween 20 in PBS) at RT for 20 min, filtered through a 35-μm nylon mesh, and diluted with 0.01% ethylenediaminetetraacetic acid (EDTA) in PBS. The PI-stained cells were analyzed by flow cytometry with the FACSVantage (Becton Dickinson, Franklin Jakes, NJ, USA). The fluorescence signals (absorbance, 620 nm) of the PI-stained cells were recorded and analyzed using CellQuest software (Becton Dickinson).

Results

Localization of Zfp318 mRNAs and proteins in mouse testis

The localization of *Zfp318* mRNAs in mouse testes was determined by *in situ* hybridization. The hybridization signal was associated with the seminiferous tubules or limited to certain populations of germ cells for a probe of short-form (Fig. 1A) and long-form (Fig. 1B) *Zfp318*, respectively. These signals were approximately equal between a probe of short-form and long-form. The long-form *Zfp318* signals were stronger than the short-form. Detailed examination of positive signals for long-form *Zfp318* revealed that *Zfp318* was localized to primary spermatocytes and in the initial steps of round spermatid formation in the seminiferous tubules (Fig. 1C) No signal was detected in spermatogonia, somatic cells, which include Sertoli cells, peritubular myoid cells, and interstitial cells (Fig. 1A, B). No hybridization signal was observed when each sense probe was used as a control. These splice variants encode two proteins, respectively, comprising 902 and 2025 amino acids (12) and containing a Cys2/His2 zinc finger motif (11). Amino acid sequence alignment and analysis revealed that ZFP318 is highly conserved in mice and humans. To determine ZFP318 localization, we performed immunohistochemistry on testis sections using the anti-human ZNF318 antibody, which recognizes homologous amino acid sequences of both mouse ZFP318 splice variants and human ZNF318 (Fig. S2, underlined, 88% homologous). Results of Western blotting analysis revealed that this anti-human ZNF318 antibody

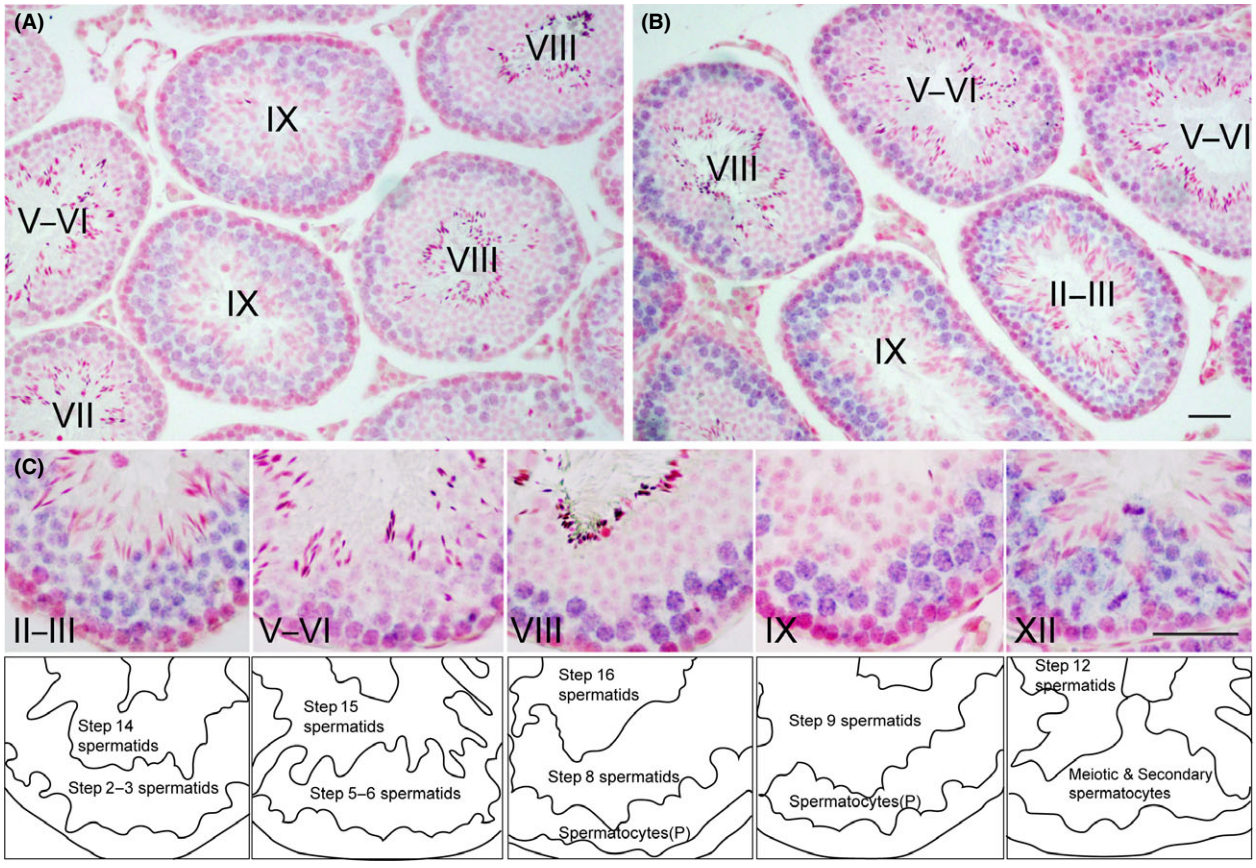

Fig. 1. Localization of *Zfp318* mRNA in testis. (A, B) *In situ* hybridization analysis of *Zfp318* mRNA localization in the testes of adult mice for a short transcript (A) and a long transcript (B). The hybridization signals (blue) are confined to the luminal compartments. (C) Higher magnification reveals that the long transcript is localized in the nuclei of pachytene spermatocytes through round spermatids. Roman numerals indicate the stage of the cycle of the mouse seminiferous epithelium. Bars: 50 μm.

recognized both the mouse ZFP318 variants, and no non-specific reaction was observed in the extract from the testis of *Zfp318*$^{-/-}$ mice (Fig. 2A). Moreover, the main variant of ZFP318 expressed in mouse testis was the long-form. Using the antibody, ZFP318 expressed inside of seminiferous tubules depending on the stages of spermatogenesis (Fig. 2B). Nucleus-restricted localization was observed in the germ cells (Figs 2B and 3). The staining intensity differed depending on the differentiation of the cells in spermatogenesis. Moderate staining was observed in primary spermatocytes from leptotene to diplotene stages, with increased intensity in the early pachytene stage (Fig. 3B, D). Interestingly, the nuclei of secondary spermatocytes, a stage between meiosis I and II and specifically stage XII in the epithelium, showed strong staining (Fig. 3F). Newly formed round spermatids, after completion of meiosis II, displayed faint nuclear staining, which was not apparent in round spermatids later in spermiogenesis, likely after step 4. Somatic cells, which include Sertoli cells, peritubular myoid cells, and interstitial cells, did not show obvious staining. Strong staining was occasionally observed in the nuclei of spermatogonia, but it was declared nonspecific since staining was also observed in the testes from *Zfp318*$^{-/-}$ mice.

Characteristics of Zfp318-null mice

To elucidate the role of *Zfp318* in spermatogenesis, we produced *Zfp318*-null using homologous recombination in ES cells (Fig. S1). Southern blot analysis of genomic DNA confirmed insertion of the targeting vector into the mutant mice (Fig. S1B). Analysis of testicular RNA and protein from *Zfp318*$^{-/-}$ mice revealed the absence of short- and long-form mRNA (Figs S1C, 2A). *Zfp318*$^{-/-}$ male mice exhibited normal health and behavior, but 129SvJ males had reduced body, testes, and epididymal weights. The testes and epididymides of *Zfp318*$^{-/-}$ mice at 10 weeks of age were significantly reduced, weighing 67.6 ± 6.9 mg (n = 10; 22.3% reduction) and 22.0 ± 5.2 mg (n = 6; 30.6%

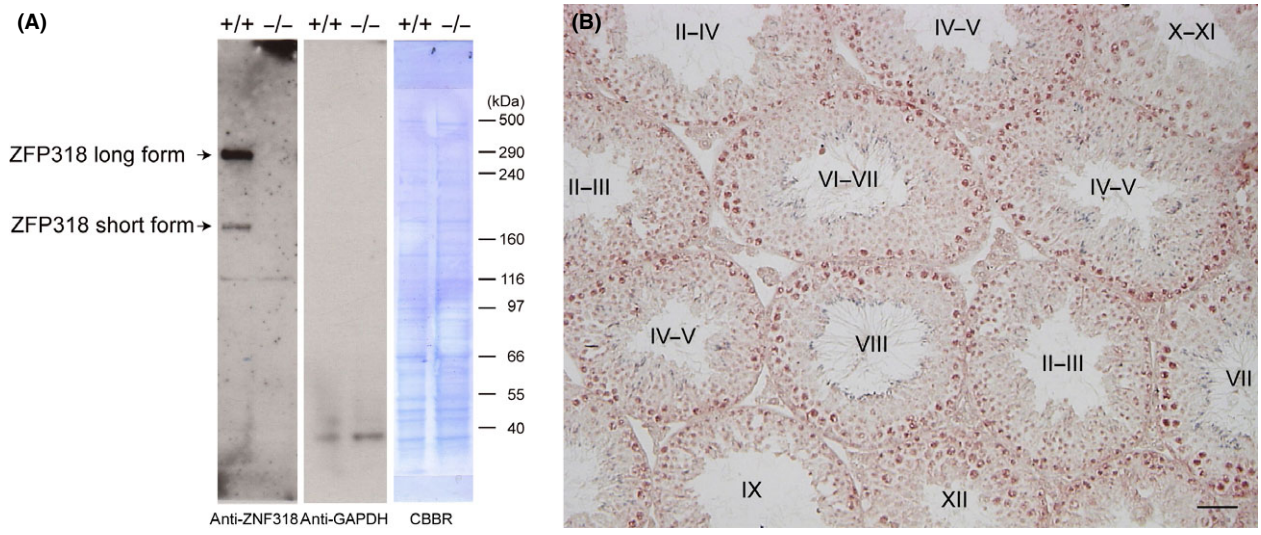

Fig. 2. Immunohistochemistry of ZFP318. (A) This antibody recognizes both forms of ZFP318 in extract from the normal adult testis. The long-form ZFP318 is the major splice variant. There is no signals in extract from the *Zfp318*$^{-/-}$ testis. Anti-GAPDH-HRP detection and CBBR (Coomassie Brilliant Blue R-250) staining of the same membrane show as a loading control. (B) Normal adult testis immunostained with the antibody and with hemotoxylin. Roman numerals indicate the stage of the cycle of the mouse seminiferous epithelium. Bar: 50 μm.

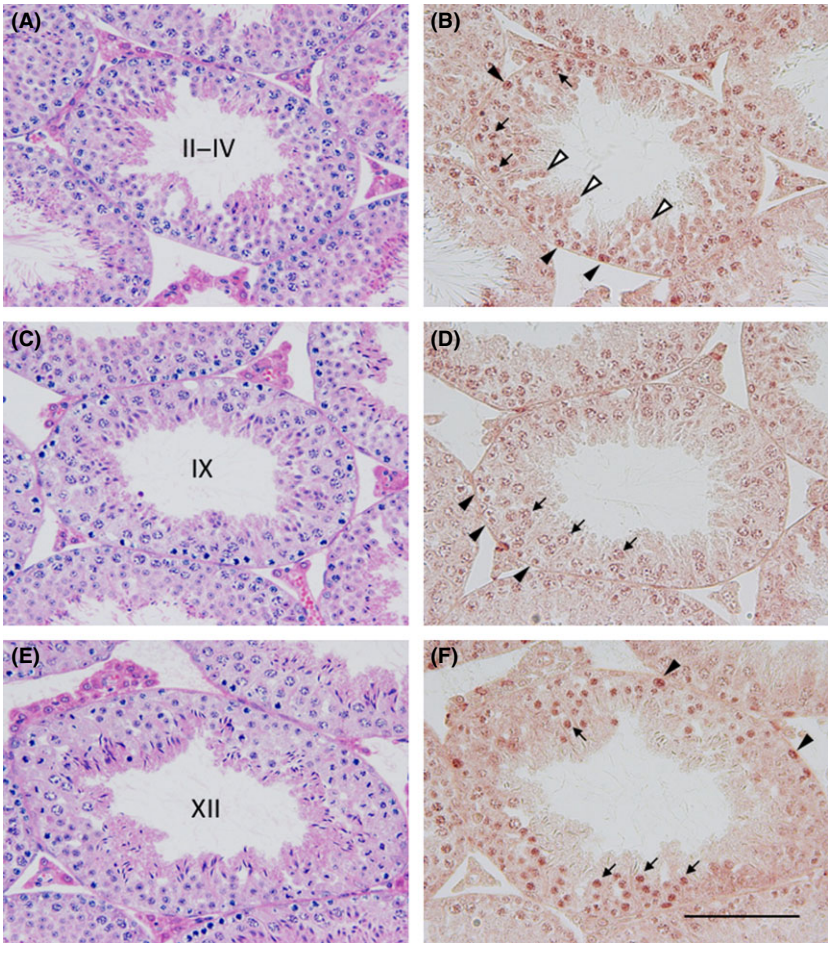

Fig. 3. Sections of the normal adult testis stained with HE (A, C and E) and the neighboring sections immunostained using an antibody against ZFP318 (B, D and F). Roman numerals reveal stage of the cycle of the mouse seminiferous epithelium. Positive signals are observed in the nuclei of spermatogonia (B and F, arrowheads), of pachytene spermatocytes (B and D, arrows) and of the secondary spermatocytes (F, arrows). Nuclei of round spermatids (B, white arrowheads) and of leptotene spermatocytes (D, arrowheads) also show weak reactions. Bar: 100 μm.

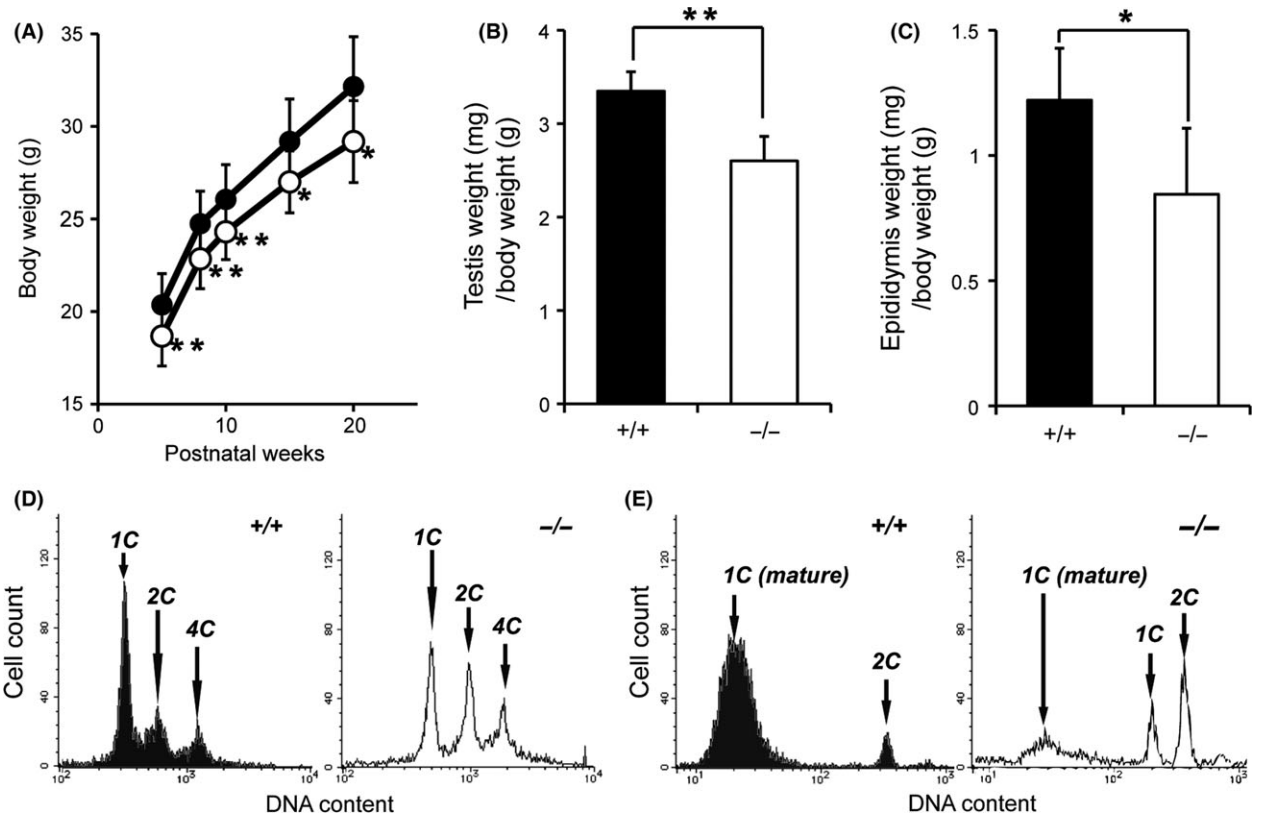

Fig. 4. *Zfp318*$^{-/-}$ male mice (129SvJ) display reduced body, testes, and epididymides weights and less mature spermatozoa. (A) *Zfp318*$^{-/-}$ mice (open circle, n = 10) display approximately 10% reduction in body weight compared to *Zfp318*$^{+/+}$ mice (closed circle, n = 10). (B) *Zfp318*$^{-/-}$ (10 weeks old) testes display ~22.3% reduction in weight (n = 10). (C) *Zfp318*$^{-/-}$ (10 weeks old) epididymides display approximately 30.8% reduction in weight (n = 6). A t-test was used for the evaluation of statistical significance. $^{*}P < 0.05$, $^{**}P < 0.001$. (D, E) Flow cytometric analysis of the DNA content of the whole testis (D) and epididymis (E). (D) 1C, haploid spermatids; 2C, diploid cells at the G1 phase of the cell cycle (mainly Sertoli cells and spermatogonia); 4C, cells at the G2 phase of the cell cycle (mainly primary spermatocytes). Each panel is representative of four or six animals, with the data averages stated in Results. (E) 1C (mature), mature haploid spermatids with condensed nuclear DNA; 1C, haploid spermatids; 2C, diploid cells at the G1 phase of the cell cycle (mainly epithelial cells of the epididymis and spermatogonia). Each panel is representative of three or four animals, with the data averages stated in Results.

reduction), respectively, when compared with those of wild-type controls, which weighted 87.0 ± 5.4 mg (n = 10) and 31.7 ± 2.4 mg (n = 5), respectively. Even when the significantly lower body weights are adjusted for (n = 10; ~10% reduction, Fig. 4A), the testes and epididymides weights of *Zfp318*$^{-/-}$ male mice remained significantly decreased (Fig. 4B, C). Furthermore, *Zfp318*$^{-/-}$ males were infertile, with complete infertility observed in 129SvJ congenics and subfertility in C57BL/6 congenics (Table 1). Therefore, 129SvJ congenic mice were used for the detailed examinations in this study.

Ratio of sperm cells in the testes and epididymides in Zfp318-null and wild-type mice

As the classical histological examination did not reveal quantitative changes between the germ cells of *Zfp318*$^{+/+}$ and *Zfp318*$^{-/-}$ mice, we performed a more rapid and sensitive analysis of germ cells by

Table 1. Fertility assessment of Zfp318-null mice

Genetic background	129SvJ			C57BL/6		
Genotype	+/+	+/–	–/–	+/+	+/–	–/–
Number of animals	10	10	11	10	10	11
Pregnancies/mated females	28/40	32/40	0/44	35/40	34/40	13/44
Average number of progeny/pregnancy	10.3	11.1	0	11.2	11.3	6.0

quantitative DNA flow cytometry. Figure 4D depicts representative histograms of PI-stained testicular cells. Based on the DNA content, three quantifiable populations were discernible: spermatids (1C), secondary spermatocytes and spermatogonia, testicular somatic cells (2C), primary spermatocytes, and G2 spermatogonia (4C). Analysis of testicular cells revealed that *Zfp318*$^{-/-}$ mice exhibited a significant decrease in 1C cells (15.4 ± 2.2% versus 19.9 ± 2.7%, $P < 0.05$) and significant increases in 2C (12.3 ± 1.7% vs 6.0 ± 2.0%, $P < 0.05$) and 4C (7.7 ± 1.0% vs 3.4 ± 0.8%, $P < 0.001$) cells when compared with *Zfp318*$^{+/+}$ mice. Figure 4E contains representative histograms of PI-stained epididymal cells. The histograms elucidated the detection of an additional population with a lower DNA content: elongated and mature spermatids (1C (mature)). Analysis of epididymal cells revealed that *Zfp318*$^{-/-}$ mice exhibited a significant decrease in 1C (mature) cells (15.7 ± 7.1% versus 37.3 ± 10.0%, $P < 0.05$) when compared with *Zfp318*$^{+/+}$ mice. A new population, which was absent from *Zfp318*$^{+/+}$ mice, called 1C (4.5 ± 1.6%), was seen in *Zfp318*$^{-/-}$ mice.

Impaired spermatogenesis in Zfp318-null mice

Histological examination of the testis revealed no obvious abnormality in the spermatogenesis of *Zfp318*$^{+/-}$ mice (data not shown). *Zfp318*$^{-/-}$ mice, however, exhibited defects in spermatogenesis (Fig. 5B, D). As spermiogenesis proceeded, fewer elongated spermatids with malformed nuclei were observed in the seminiferous epithelium. Vacuoles were sporadically observed in the epithelium, indicating degeneration

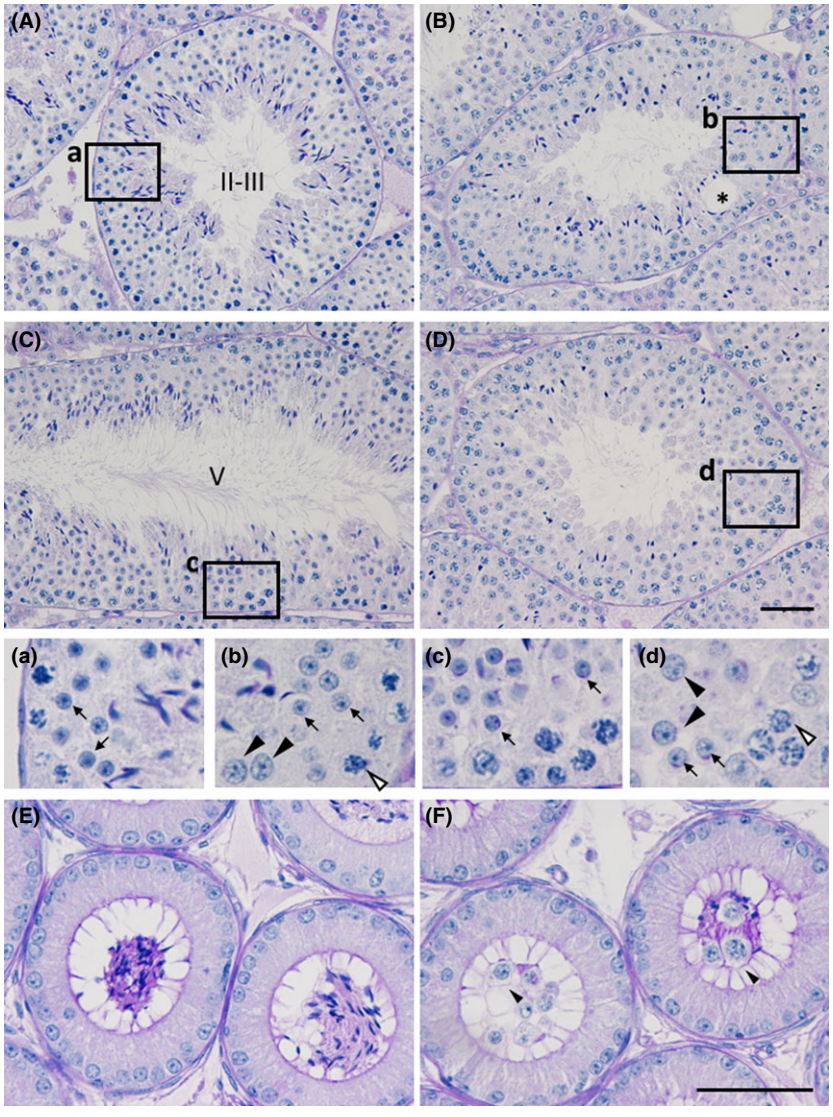

Fig. 5. Histological analysis of testes and epididymides of the *Zfp318*$^{-/-}$ mouse. PAS-hematoxylin-stained sections of testes (A-D) and caput epididymides (E and F). Depicted areas in A–D are enlarged in a–d, respectively. Roman numerals in A and C show the stage of the cycle of the mouse seminiferous epithelium. Seminiferous tubules in B and D were regarded as the corresponding stage of A and C, respectively. The wild-type male shows normal testicular morphology (A and C), whereas the mutant testis shows affected spermatogenesis including vacuole formation (B, asterisk) and sparsely located elongated spermatids (D). Note the cells with the large nuclei (b and d, arrowheads) among the normal round spermatids (arrows), comparable to those of pachytene spermatocytes (b and d, white arrowheads). Accumulation of the sperm is seen in the lumen of the wild-type epididymal duct (E). Sloughed germ cells with few sperm are observed in the mutant (F). Bars: 50 μm.

and dissolution of germ cells (Fig. 5B). Additionally, irregular sized nuclei with similar morphology to those of the round spermatids were detected in the layer of the spermatids in the epithelium (Fig. 5a–d). The nuclear diameter of the cells was comparable to those of pachytene spermatocytes that co-existed in the epithelium. The abnormal cells with larger nuclei, evaluated mainly by the co-existing spermatogonia and spermatocytes, were detected in the epithelium at stages I to V of the cycle, but not in the later stages of the epithelium. The impaired spermatogenesis of the mutant mice was evidenced with little accumulation of the sperm containing sloughed germ cells in the lumen of the epididymal duct (Fig. 5F).

Discussion

We generated and analyzed the male reproductive phenotype of *Zfp318-null mice*, and the results indicate that the gene is indispensable for proper spermatogenesis, and hence, male fertility. Spermatogenesis proceeded normally up to the meiosis prophase just before the spermatozoa morphogenesis steps. Round to elongated spermatids exhibited nuclear malformation from the first step onwards, and completed spermatozoa were decreased in number. We have previously demonstrated that *Zfp318* germ cell-specific transcripts first appear at post-natal day 16, as spermatocytes enter meiotic prophase (Ishizuka *et al.* 2003). In this study, the expression of these transcripts was observed from pachytene spermatocytes at meiotic prophase to the initial steps of round spermatids in seminiferous tubules, suggesting that *Zfp318* is involved primarily in meiosis, and the protein expression had the same distribution. The nuclei of secondary spermatocytes showed strong staining, which was diminished in the later stages of round spermatids and elongated spermatids. Therefore, ZFP318 was not a component of spermatozoa but may act as a regulatory factor of meiosis or a transcriptional factor of genes required in spermiogenesis. Because no developmental difference was observed until that of secondary spermatocytes between wild-type and *Zfp318-null* testes, the essential role of ZFP318 in spermatogenesis appears to involve meiosis. Quantitative DNA flow cytometry was conducted to further investigate the role of ZFP318 in the regulation of spermatogenesis. The quantities of primary (4C) and secondary (2C) spermatocytes increased, while spermatids (1C) decreased. Histological examination also revealed the morphological changes related to this phenomenon, including irregularly sized nuclei of the round spermatids and malformation of the nuclei of spermatids. These results also suggest a meiosis-promoting function of the gene.

The two splice variants of *Zfp318* are nuclear proteins that alternatively function as coactivator and corepressor of AR (Tao *et al.* 2006a). However, the deletion of the AR gene in mouse germ cells does not affect spermatogenesis and male fertility (Wang *et al.* 2009). AR-mediated transcriptional activation in germ cells is not essential for spermatogenesis. Western blotting showed that both the splice variants of *Zfp318* were expressed in testicular germ cells, with the main variant being the long-form. These results suggest that long-form homodimers of ZFP318 could be part of a coactivator complex for transcriptional activation of nuclear receptors other than AR. ZFP318 has one (short-form) or two (long-form) U-1 like zinc finger domains which can directly bind to DNA without AR. Moreover, once considered to function exclusively as sequence-specific DNA-binding motifs, zinc-fingers are now known to also recognize RNA and other proteins (Gamsjaeger *et al.* 2007). Recently, *Zfp318* was identified by genetic screen in mice as a transacting factor responsible for expression of IgD, the alternatively spliced Igh product made by mature B lymphocytes (Enders *et al.* 2014; Pioli *et al.* 2014). Indeed, our *Zfp318-null* mice extinguished IgD expression on mature B cells and increased IgM (Enders *et al.* 2014). ZFP318 also has a conserved domain concerning chromosome segregation protein (PRK03918) or tumor suppressor, trichoplein or mitostatin, was first defined as a meiosis-specific nuclear structural protein (pfam13868) (Vecchione *et al.* 2009), which has a crucial role in MT-anchoring activity at the centrosome in proliferating cells (Ibi *et al.* 2011). Although ZFP318 seems to play an important role progressing meiosis in spermatogenesis, further study will be need to show if ZFP318 functions as a meiosis-specific nuclear structural protein.

Acknowledgments

We would like to thank H. Nishimura, K. Takada, S. Kasagi, T. Yokoyama, H. Yumiyama, K. Sasaki, S. Kamakura, K. Yamasaki, T. Inoue, and A. Kurotobi for their help in the maintenance of mice and K. Nunoichi and Y. Maruyama for their technical assistance in producing the $Zfp318^{-/-}$ mice. This work was supported by Grants-in-Aid for Scientific Research from the Ministry of Education, Science, Sports, and Culture of Japan and by grants from the Promotion and Mutual Aid Corporation for Private Schools of Japan.

References

Ballow, D., Meistrich, M. L., Matzuk, M. & Rajkovic, A. 2006. Sohlh1 is essential for spermatogonial differentiation. *Dev. Biol.* **294**, 161–167.

Blendy, J. A., Kaestner, K. H., Weinbauer, G. F., Nieschlag, E. & Schutz, G. 1996. Severe impairment of spermatogenesis in mice lacking the CREM gene. *Nature* **380**, 162–165.

Buaas, F. W., Kirsh, A. L., Sharma, M., Mclean, D. J., Morris, J. L., Griswold, M. D., De Rooij, D. G. & Braun, R. E. 2004. Plzf is required in adult male germ cells for stem cell self-renewal. *Nat. Genet.* **36**, 647–652.

Chizaki, R., Yao, I., Katano, T., Matsuda, T. & Ito, S. 2012. Restricted expression of Ovol2/MOVO in XY body of mouse spermatocytes at the pachytene stage. *J. Androl.* **33**, 277–286.

Costoya, J. A., Hobbs, R. M., Barna, M., Cattoretti, G., Manova, K., Sukhwani, M., Orwig, K. E., Wolgemuth, D. J. & Pandolfi, P. P. 2004. Essential role of Plzf in maintenance of spermatogonial stem cells. *Nat. Genet.* **36**, 653–659.

Eddy, E. M. 2002. Male germ cell gene expression. *Recent Prog. Horm. Res.* **57**, 103–128.

Enders, A., Short, A., Miosge, L. A., Bergmann, H., Sontani, Y., Bertram, E. M., Whittle, B., Balakishnan, B., Yoshida, K., Sjollema, G., Field, M. A., Andrews, T. D., Hagiwara, H. & Goodnow, C. C. 2014. Zinc-finger protein ZFP318 is essential for expression of IgD, the alternatively spliced Igh product made by mature B lymphocytes. *Proc. Natl. Acad. Sci. U S A.* **111**, 4513–4518.

Gamsjaeger, R., Liew, C. K., Loughlin, F. E., Crossley, M. & Mackay, J. P. 2007. Sticky fingers: zinc-fingers as protein-recognition motifs. *Trends Biochem. Sci.* **32**, 63–70.

Ibi, M., Zou, P., Inoko, A., Shiromizu, T., Matsuyama, M., Hayashi, Y., Enomoto, M., Mori, D., Hirotsune, S., Kiyono, T., Tsukita, S., Goto, H. & Inagaki, M. 2011. Trichoplein controls microtubule anchoring at the centrosome by binding to Odf2 and ninein. *J. Cell Sci.* **124**, 857–864.

Inoue, A., Ishiji, A., Kasagi, S., Ishizuka, M., Hirose, S., Baba, T. & Hagiwara, H. 2000. The transcript for a novel protein with a zinc finger motif is expressed at specific stages of mouse spermatogenesis. *Biochem. Biophys. Res. Commun.* **273**, 398–403.

Ishizuka, M., Ohshima, H., Tamura, N., Nakada, T., Inoue, A., Hirose, S. & Hagiwara, H. 2003. Molecular cloning and characteristics of a novel zinc finger protein and its splice variant whose transcripts are expressed during spermatogenesis. *Biochem. Biophys. Res. Commun.* **301**, 1079–1085.

Ishizuka, M., Kawate, H., Takayanagi, R., Ohshima, H., Tao, R. H. & Hagiwara, H. 2005. A zinc finger protein TZF is a novel corepressor of androgen receptor. *Biochem. Biophys. Res. Commun.* **331**, 1025–1031.

Krishnamurthy, H., Weinbauer, G. F., Aslam, H., Yeung, C. H. & Nieschlag, E. 1998. Quantification of apoptotic testicular germ cells in normal and methoxyacetic acid-treated mice as determined by flow cytometry. *J. Androl.* **19**, 710–717.

Krishnamurthy, H., Danilovich, N., Morales, C. R. & Sairam, M. R. 2000. Qualitative and quantitative decline in spermatogenesis of the follicle-stimulating hormone receptor knockout (FORKO) mouse. *Biol. Reprod.* **62**, 1146–1159.

Martianov, I., Fimia, G. M., Dierich, A., Parvinen, M., Sassone-Corsi, P. & Davidson, I. 2001. Late arrest of spermiogenesis and germ cell apoptosis in mice lacking the TBP-like TLF/TRF2 gene. *Mol. Cell* **7**, 509–515.

Nantel, F., Monaco, L., Foulkes, N. S., Masquilier, D., Lemeur, M., Henriksen, K., Dierich, A., Parvinen, M. & Sassone-Corsi, P. 1996. Spermiogenesis deficiency and germ-cell apoptosis in CREM-mutant mice. *Nature* **380**, 159–162.

Pioli, P. D., Debnath, I., Weis, J. J. & Weis, J. H. 2014. Zfp318 regulates IgD expression by abrogating transcription termination within the Ighm/Ighd locus. *J. Immunol.* **193**, 2546–2553.

Raverot, G., Weiss, J., Park, S. Y., Hurley, L. & Jameson, J. L. 2005. Sox3 expression in undifferentiated spermatogonia is required for the progression of spermatogenesis. *Dev. Biol.* **283**, 215–225.

Russell, L. D., Ettlin, R. A., Sinha Hikim, A. P. & Clegg, E. D. 1990. *Histological and Histopathological Evaluation of the Testis*. Clearwater, Fl, USA, Cache River Press.

Sassone-Corsi, P. 1997. Transcriptional checkpoints determining the fate of male germ cells. *Cell* **88**, 163–166.

Tao, R. H., Kawate, H., Ohnaka, K., Ishizuka, M., Hagiwara, H. & Takayanagi, R. 2006a. Opposite effects of alternative TZF spliced variants on androgen receptor. *Biochem. Biophys. Res. Commun.* **341**, 515–521.

Tao, R. H., Kawate, H., Wu, Y., Ohnaka, K., Ishizuka, M., Inoue, A., Hagiwara, H. & Takayanagi, R. 2006b. Testicular zinc finger protein recruits histone deacetylase 2 and suppresses the transactivation function and intranuclear foci formation of agonist-bound androgen receptor competitively with TIF2. *Mol. Cell. Endocrinol.* **247**, 150–165.

Vecchione, A., Fassan, M., Anesti, V., Morrione, A., Goldoni, S., Baldassarre, G., Byrne, D., D'arca, D., Palazzo, J. P., Lloyd, J., Scorrano, L., Gomella, L. G., Iozzo, R. V. & Baffa, R. 2009. MITOSTATIN, a putative tumor suppressor on chromosome 12q24.1, is downregulated in human bladder and breast cancer. *Oncogene* **28**, 257–269.

Wang, R. S., Yeh, S., Tzeng, C. R. & Chang, C. 2009. Androgen receptor roles in spermatogenesis and fertility: lessons from testicular cell-specific androgen receptor knockout mice. *Endocr. Rev.* **30**, 119–132.

Weiss, J., Meeks, J. J., Hurley, L., Raverot, G., Frassetto, A. & Jameson, J. L. 2003. Sox3 is required for gonadal function, but not sex determination, in males and females. *Mol. Cell. Biol.* **23**, 8084–8091.

Yan, W., Si, Y., Slaymaker, S., Li, J., Zheng, H., Young, D. L., Aslanian, A., Saunders, L., Verdin, E. & Charo, I. F. 2010. Zmynd15 encodes a histone deacetylase-dependent transcriptional repressor essential for spermiogenesis and male fertility. *J. Biol. Chem.* **285**, 31418–31426.

Yoshimura, T., Toyoda, S., Kuramochi-Miyagawa, S., Miyazaki, T., Miyazaki, S., Tashiro, F., Yamato, E., Nakano, T. & Miyazaki, J. 2009. Gtsf1/Cue110, a gene encoding a protein with two copies of a CHHC Zn-finger motif, is involved in spermatogenesis and retrotransposon suppression in murine testes. *Dev. Biol.* **335**, 216–227.

Zhou, H., Liu, L. H., Zhang, H., Lei, Z. & Lan, Z. J. 2010. Expression of zinc finger protein 105 in the testis and its role in male fertility. *Mol. Reprod. Dev.* **77**, 511–520.

Supporting Information

Additional Supporting Information may be found online in the supporting information tab for this article:

Fig. S1. *Zfp318* knockout scheme and validation.

Fig. S2. Amino acid sequences of human ZNF318 (NP_055160), murine ZFP318 isoform 1 (long-form) (NP_997554), and murine ZFP318 isoform 2 (short-form) (NP_067321).